ACCOUNTS
of chemical research

Nanoscale Quantitative Measurement of the Potential of Charged Nanostructures by Electrostatic and Kelvin Probe Force Microscopy: Unraveling Electronic Processes in Complex Materials

ANDREA LISCIO,[†] VINCENZO PALERMO,[†,*] AND PAOLO SAMORÌ[‡,*]

[†]*Istituto per la Sintesi Organica e la Fotoreattività, Consiglio Nazionale delle Ricerche, via Gobetti 101, 40129 Bologna, Italy, and* [‡]*Nanochemistry Laboratory, ISIS - CNRS 7006, Universite de Strasbourg, 8 allee Gaspard Monge, 67000 Strasbourg, France*

RECEIVED ON SEPTEMBER 25, 2009

CONSPECTUS

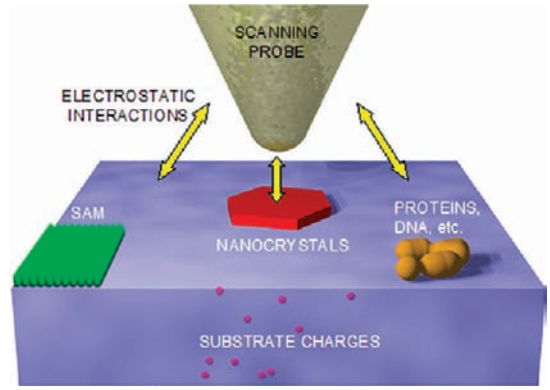

In microelectronics and biology, many fundamental processes involve the exchange of charges between small objects, such as nanocrystals in photovoltaic blends or individual proteins in photosynthetic reactions. Because these nanoscale electronic processes strongly depend on the structure of the electroactive assemblies, a detailed understanding of these phenomena requires unraveling the relationship between the structure of the nano-object and its electronic function. Because of the fragility of the structures involved and the dynamic variance of the electric potential of each nanostructure during the charge generation and transport processes, understanding this structure−function relationship represents a great challenge.

This Account discusses how our group and others have exploited scanning probe microscopy based approaches beyond imaging, particularly Kelvin probe force microscopy (KPFM), to map the potential of different nanostructures with a spatial and voltage resolution of a few nanometers and millivolts, respectively. We describe in detail how these techniques can provide researchers several types of chemical information. First, KPFM allows researchers to visualize the photogeneration and splitting of several unitary charges between well-defined nano-objects having complementary electron-acceptor and -donor properties. In addition, this method maps charge injection and transport in thin layers of polycrystalline materials. Finally, KPFM can monitor the activity of immobilized chemical components of natural photosynthetic systems.

In particular, researchers can use KPFM to measure the electric potential without physical contact between the tip and the nanostructure studied. These measurements exploit long-range electrostatic interactions between the scanning probe and the sample, which scale with the square of the probe−sample distance, d. While allowing minimal perturbation, these long-range interactions limit the resolution attainable in the measurement of potentials. Although the spatial resolution of KPFM is on the nanometer scale, it is inferior to that of other related techniques such as atomic force or scanning tunneling microscopy, which are based on short-range interactions scaling as d^{-7} or e^{-d}, respectively. To overcome this problem, we have recently devised deconvolution procedures that allow us to quantify the electric potential of a nano-object removing the artifacts due to its nanometric size.

Published on the Web 01/08/2010 www.pubs.acs.org/acr
10.1021/ar900247p

I. Introduction

Kelvin probe force microscopy (KPFM),[1,2] also known as Kelvin probe microscopy (KPM) or scanning Kelvin probe microscopy (SKPM), is a scanning probe technique based on dynamic force microscopy mapping simultaneously both surface morphology and electric potential of nano-objects with high spatial and electrical resolution (Figure 1a).

KPFM is a combination of the macroscopic Kelvin probe technique, introduced by Lord Kelvin in 1898[3] (using the vibrating capacitance setup[4]), and atomic force microscopy (AFM).[5] It uses a conductive probe as an electrode to determine the work function, ϕ_s, of a metal substrate.[6] This is attained by measuring the local surface potential difference (ΔSP) between a probe with known work function, ϕ_p, and the sample, $\Delta SP = (\phi_p - \phi_s)/q$, where q is the elementary charge. In the case of semiconductor and dielectric samples, the potential of the material depends upon surface charge, upon dopant charges typically existing both on and beneath the surface, and upon polarization effects.[7]

Over the past two decades, KPFM has become an important instrument for studying the electronic properties of small structures down to the nanometer scale. KPFM was successfully employed to investigate a wide range of systems,[8] including inorganic[9] and organic thin films[10,11] as well as proteins,[12,13] over multiple length scales, from meso- to nanoscopic levels. It has also allowed the measurement of the charging and discharging processes of single, isolated molecules.[14] Of technological relevance, KPFM has proven to be a viable tool for exploring the dynamic properties of working electronic devices.[15−21] Among others, it made it possible both to map photocharge density variations in donor−acceptor blends at surfaces[16,22−24] and to directly measure the potential drops for different source and gate voltages in organic field-effect transistors (OFETs).[15,17,25,26]

Although the physical principle on which KPFM is based is quite simple,[27,28] the achievement of high spatial and potential resolution in a reliable and reproducible manner is not straightforward. This Account aims at elucidating the physicochemical meaning of the measurements of the electric potential of *nanoscopic* objects, which can significantly differ from that of *macroscopic* objects. To this end, we will provide examples of recent quantitative KPFM explorations of complex systems, phenomena, and devices mostly based on abiotic systems.

What is the potential of a nanometric object and how can it be measured with high precision? To explain this, we need to consider the two extreme cases: (i) single-molecule layers on metal surfaces and (ii) thick layers (hundreds of nanometers).

On the one hand, the chemisorbed self-assembled monolayers (SAMs) are uniform organic adlayers. They can be obtained by simply immersing a Au substrate in a solution of thiol-functionalized R−SH molecules.[29] Similarly, silica surfaces can be functionalized with organic SAMs using silane chemistry. The chemical, physical, and electronic properties of SAMs have been extensively studied, particularly in the field of organic electronics where they are employed to modify the electrode ϕ. In fact, SAMs are often used to modify the potential of the surface (SP_{surf}), which becomes the result of contributions from both substrate and adsorbed monolayer:[18]

$$SP_{surf} = SP_{substrate} + \mu_{SAM}/q + \Delta_{bond} \quad (1)$$

where μ_{SAM} is the effective molecular dipole perpendicular to the substrate and Δ_{bond} is the interfacial bond due to the rearrangement of electron density at the substrate−SAM interface.

In the case of thicker organic layers (d > 100 nm, for example, active layers of OFET and solar cells), however, the influence of the underlying substrate is normally neglected.

Between these two extreme cases, at intermediate thicknesses, both the deposited material and substrate potentials can contribute to the resulting SP. Moreover, in the case of semiconducting films, charge density variations can be measured on increasing the film thickness due to band-bending.

The study of molecular films several tens of nanometers thick is not only of fundamental scientific interest, but also important technologically. For example, in OFETs the active channel is confined to a few monolayers at the organic−dielectric interface. If one wants to measure the true electric potential of such thin layers, it is important to understand the influence of the underlying substrate. In the case of organic solar cells, despite the high thickness, which allows one to neglect the substrate contribution, the organic films consist of a phase-segregated blend of electron acceptor (EA) and electron donor (ED) materials having different HOMO−LUMO levels. The exciton generated by light absorption diffuses toward the interface between the two phases, leading to charge separation with the generation of electrons and holes. For optimum performance, EA and ED should exhibit phase segregation on the 5−10 nm scale, namely, the scale addressable by scanning probe techniques.[30] In particular, the charge generation at the interface can be easily visualized and correlated with the morphology by KPFM.[22,23] Spatial and voltage resolution are crucial for reliable observation of the smallest features, because the typical EA/ED intermixing is

usually comparable to or even smaller than KPFM resolution. In this way, the probe senses the potential of both materials intermixed on the surface, yielding a potential that is the weighted average of all the contributing potentials.

These remarks are not unique to the study of organic materials but are of importance for any structure featuring a vertical or lateral size smaller than a few tens of nanometers.

Overall, the general questions addressed in this Account are as follows:

(1) How can one determine the contribution of the substrate in a work function measurement of an adsorbed organic material?

(2) In the measurement of nano-objects, approaching the KPFM resolution limit, is it possible to reconstruct the *real* nanostructure potential by removing the influence of the surrounding substrate?

Once these fundamental questions have been addressed, we will show how KPFM can be successfully employed to unravel complex electronic processes and phenomena in natural systems and in electronic devices.

II. Description of the KPFM Technique

KPFM measures the electrostatic interactions between the sample and a vibrating conductive probe mounted at the edge of a cantilever, whose swing is induced by an alternating bias (V_{AC}) with frequency ω (Figure 1a). Starting from two electrodes, probe and sample with a given ϕ (Figure 1b), upon contact during measurement their Fermi levels align causing an electrostatic force that depends on the SP difference (Figure 1c). The ω-term of the electrostatic force (F_ω) depends on the ΔSP giving $F_\omega(t) = (dC/dz)(V_{DC} - \Delta SP)V_{AC} \sin(\omega t)$, where C is the probe−sample capacitance. This F_ω force causes the oscillation of the probe, which is detected by a photodiode. In electrostatic force microscopy (EFM), F_ω is directly measured using a lock-in amplifier to isolate the ω-frequency signal. If both probe and sample are grounded (i.e., $V_{DC} = 0$), F_ω is proportional to ΔSP, but its value cannot be determined exactly because calculating the dC/dz term would require a detailed knowledge of system properties and probe−sample geometry. This limitation disappears in KPFM measurements, where a further V_{DC} is applied to the probe by a feedback circuit to nullify F_ω and thus obtain $V_{DC} = \Delta$SP (Figure 1d,e). Hence, by scanning the probe over the surface, one can obtain a 2D map of the SP of the sample. The above-described principle is common to all KPFM instruments, although different modes are employed. A detailed discussion of these methods is available in ref 31.

In KPFM measurements of conductive samples, probe−sample interaction is due only to Fermi level alignment; thus the measured ΔSP is simply the probe−sample ϕ difference. But what is the physical meaning of KPFM measurements of nonconductive nanostructures, in which charges are trapped on the surface or within the substrate?

The description employed for conductive samples includes metals and highly doped semiconductors (Figure 1d, flatband case). Conversely, for samples with decreased doping levels and for dielectric samples, other terms have to be considered.[32]

In general, the local SP is due to the charge density on the sample surface as expressed by the Poisson equation. The SP depends on the presence of surface or bulk charges, on surface dipoles, and on the interfacial electronic states in the heterostructures (Figure 1e).

In general, the effect of surface SAMs is modeled as an oriented dipole, to be added to the substrate SP, which could, in principle, be calculated from the dipole of the single molecules and on their density in the SAM.[33] In the case of thicker layers, however, a precise orientation of the molecular dipoles can no longer be assumed; the SP changes smoothly with layer thickness, due usually to the presence of band-bending. The SP varies until the thickness is smaller than the semiconductor space charge layer depending on the charge density of the material. For greater thicknesses, the SP can be considered as the bulk value and as independent of the substrate. It was experimentally observed that the ϕ of a C_{60} film on metal electrodes varies with the thickness in the space charge layer, becoming completely independent in fairly thick (higher than 100 nm) films.

One of the main sources of experimental artifacts is ascribable to the finite size of the probe and its shape, which limit the maximum achievable resolution of KPFM causing an underestimation of the measured potential with respect to the real value. KPFM measurements sense a data set of electrostatic forces between the scanning probe and the area of the sample below. Due to the long-range nature of electrostatic interactions, the area of the sampled surface in such a measurement expands to several tens of nanometers beyond the area beneath the probe tip. Moreover, the surrounding part of the conical probe and the oscillating cantilever also contribute to the interaction. This artifact is mainly due to the ω-signal, which depends on both the tip−sample distance and the capacitance gradient. Lee et al.[34] proposed correcting the artifacts due to sample roughness (i.e., topographical effects) by separating the ω and 2ω terms of the cantilever response. With nanoscale objects, their size is comparable to that of the

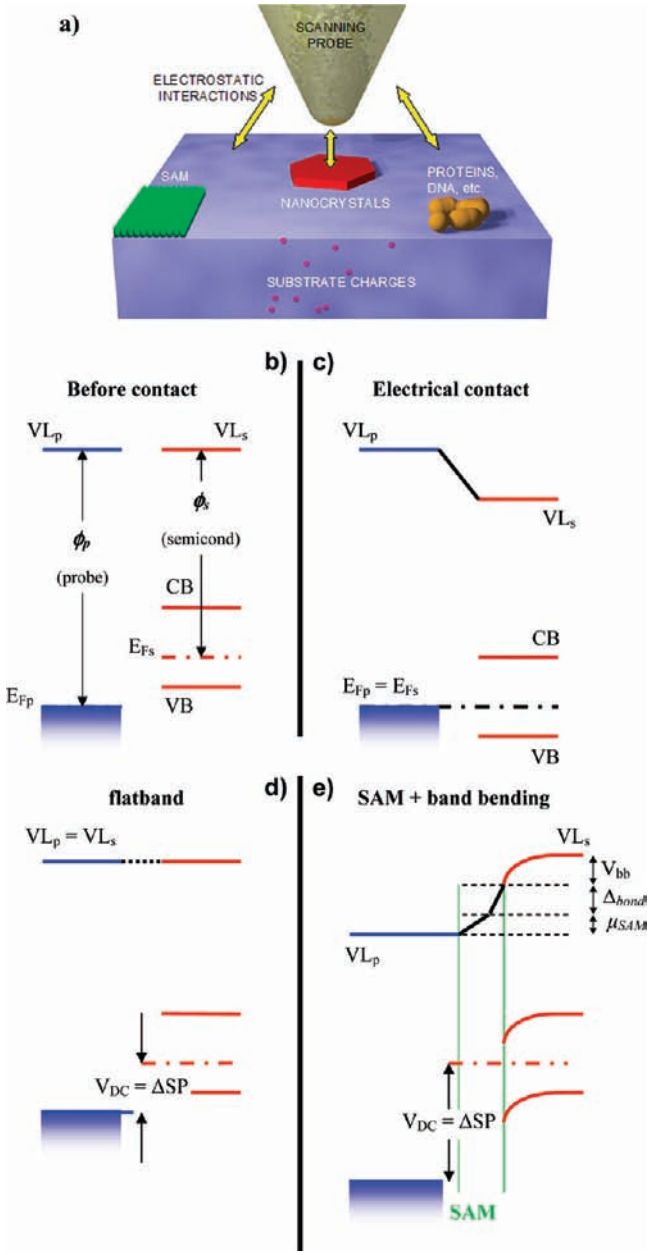

FIGURE 1. (a) Scheme of the principle of KPFM on nano-objects. (b, c) Schematic of *Z*-direction energy bands for the probe−surface syste: (b) probe (blue) and semiconductor sample (red) have different Fermi levels (E_F), which (c) are aligned when the two materials are electrically contacted. (d) When $V_{DC} = \Delta SP$ is applied, the two vacuum levels (VL) align, nullifying the work−function difference (i.e., the flatband case). (e) In the real case, several terms contribute to ΔSP including band-bending (V_{bb}), the interface dipole (Δ_{bond}), and the SAM dipoles (μ_{SAM}).

probe and the contribution of the substrate, as well as the surrounding structures, plays an important role.

Here, we focus upon these artifacts showing that they are strongly correlated with the KPFM measurement itself and their evaluation is necessary to study the surfaces of nanostructured systems.

The surface area of the sample interacting with the probe is defined as the *effective area*.[35] The local potential of the whole surface within this area contributes to the measured SP. The estimation of the highest lateral resolution (LR) attainable by KPFM is strictly related to the quantification of the effective area. The AFM technique is governed by van der Waals interactions having a short range of a few nanometers (the attractive force is proportional to d^{-7}, where d is the distance between the two interacting bodies); this assumes that only the probe apex interacts with the sample surface. On the other hand, KPFM measurements are governed by long-range Coulombic interactions proportional to d^{-2}; thus the contribution of the probe and the cantilever cannot be neglected. This problem is common to other scanning probe techniques relying on long-range physical properties, such as EFM or magnetic force microscopy. When the size of the nanostructures is smaller or even comparable to the LR of the instrument, measurement of the true nanostructure potential is not straightforward. Moreover, LR is not an unambiguous definition, being strictly connected to the morphology of the system studied. According to Rayleigh's criterion, it can be defined in two different ways: (i) the minimum detectable distance between two distinct objects or (ii) the apparent measured size of the minimum detectable isolated structure.

Both LR and the effective area can be parametrized using a *transfer function* (Γ), also called point spread function, a mathematical representation of the relation between the input (the real SP profile, SP_0) and the output (the measured SP profile) signals. The output is given by a convolution between SP_0 and Γ, which contains all the electrical and geometrical details of the probe−sample interactions (Figure 2), and its description becomes the main issue of KPFM measurements.

This problem was approached in two different ways: (i) by using an analytical algorithm describing the probe as a well-defined geometrical structure (a sphere, a truncated cone, etc.) to model its interaction with the sample[36,37] or (ii) by simulating with finite-element analysis the effective force.[38]

In previous work,[39] we showed how deconvolution artifacts and the effects of finite probe size can be accounted for by combining AFM and KPFM data obtained over the same area to quantify the measured volume, independent of nanostructure size. This procedure was tested on a real system (P3HT nanofibers of different size), as detailed below.

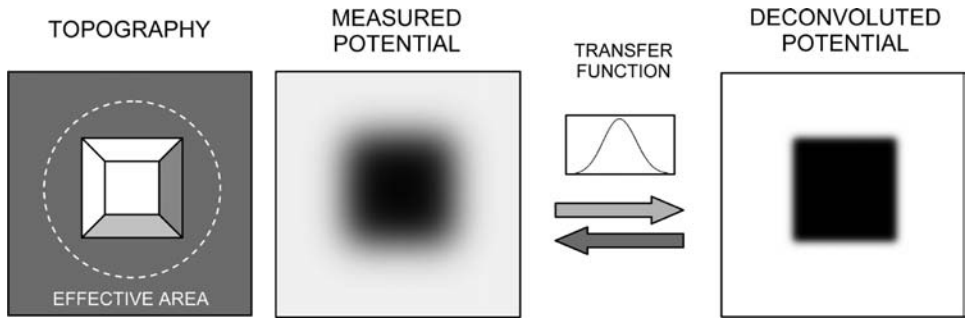

FIGURE 2. The measured SP image is described as the convolution between the real potential of the sample and the transfer function of the microscope.

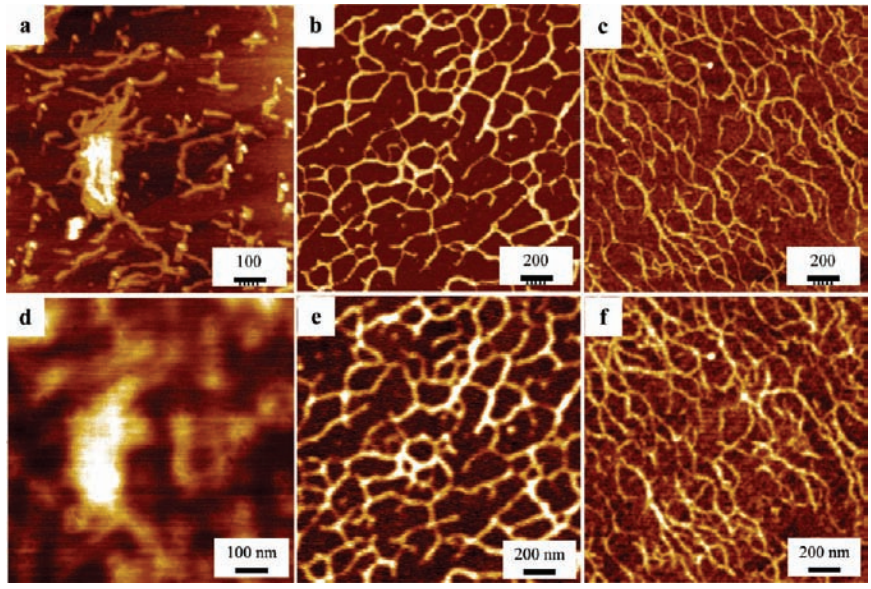

FIGURE 3. AFM topography and corresponding KPFM images of P3HT fibers deposited on (a,d) HOPG, (b,e) mica, and (c,f) silica. *Z*-ranges were (a) 9 nm, (b) 6 nm, (c) 6 nm, (d) 120 mV, (e) 60 mV, and (f) 50 mV. Reproduced with permission from ref 39. Copyright 2008 Wiley-VCH.

III. Application of KPFM to the Measurement of Real Nano-objects

In the case of well-defined nanostructures, it is possible to reconstruct Γ by comparing the broadening of the SP profiles directly from the measured KPFM images.[35,39,40] Polymer networks having weak interactions with the substrate are quasi-1D systems ideal for testing this approach because they form well-defined, highly reproducible fibers on the substrate of varying nanometric sizes.

We recently studied the self-assembly of regioregular poly(3-hexylthiophene) (P3HT) fibers deposited on flat surfaces from $CHCl_3$ solutions.[39] Figure 3 shows the topographic AFM and corresponding KPFM images of P3HT deposited on highly oriented pyrolytic graphite (HOPG), muscovite mica, and silica. The different lamellar packing can be principally ascribed to the different solvent wettability of the substrates. All the substrates exhibit darker areas in the potential image, whereas the fibers are brighter. For the sake of simplicity, all the P3HT SPs are referred to the potential of the uncovered substrate areas ($SP_{substrate} = 0$), larger than the effective area, amounting to ~150 nm for the setup used. The correlation plots are between the measured SPs and the corresponding fiber sizes for all three substrates (Figure 4a). The decrease in the P3HT SP with the width of the architecture is a purely geometrical artifact due to the above-mentioned convolution effects. The measured P3HT SP is an average of both fiber and substrate potential, because the widths of the bundles are smaller than the effective area. Similarly, a monotonic trend of the HOPG SP is measured with the increasing size of the uncovered area with an asymptotic value tending to zero (Figure 4b).

Our model allows separation of P3HT and substrate contributions, reproducing the measured monotonic trend of the HOPG SP (red line in Figure 4b). After deconvolution, the bun-

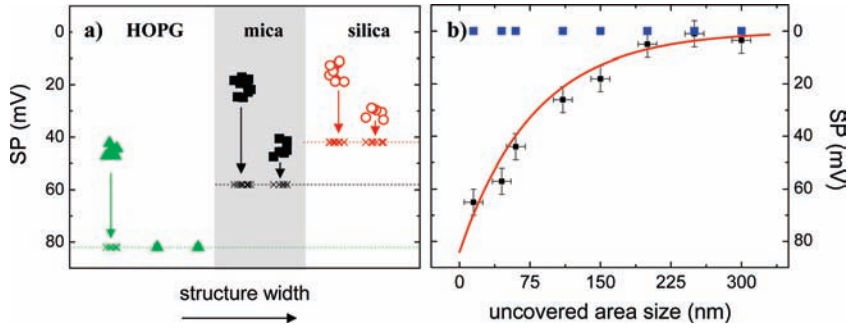

FIGURE 4. (a) Measured SP values corresponding to the different P3HT structures on HOPG (▲), mica (■), and silica (○) having different widths. The variation of the measured SPs of the nano-objects is calculated by using the convolution procedure, and the asymptotic SP values are displayed (dashed line) for each substrate. (b) Dependence of measured (■) and simulated (—) SP on the size of the uncovered HOPG surface area. The asymptotic SP values are reported using blue dots. Reproduced with permission from ref 39. Copyright 2008 Wiley-VCH.

dles and substrate SPs are independent of the sizes (blue dots for HOPG). More details on the deconvolution procedure employed can be found in ref 39.

The electronic properties of a solid depend on its structure at the atomic scale. One of the most impressive examples is given by the allotropic forms of carbon, which can be conducting (HOPG) or insulating (diamond). Similar behavior has been observed on supramolecular assemblies. Molecular-architecture SP depends on the interaction between adjacent molecules, as seen in eq 1 for the case of a SAM. Brédas et al.[41] showed that, especially in the case of conjugated molecules, the change in the intermolecular stacking distance of a few angstroms can cause shifts in the HOMO and LUMO of up to 1 eV. Thus, the conduction−valence band of a nanocrystal or nanofiber made of stacked molecules can differ significantly from the HOMO−LUMO levels of the free molecule.

The effects of different intermolecular stacking upon the ϕ of a nanostructure was investigated by comparing the SP of crystalline assemblies of perylene−bis(dicarboximide) (PDI) with architectures obtained from perylene−bis(dicarboximide)-functionalized poly(isocyanopeptide) (P-PDI) polymers. In P-PDI, the perylene units tend to stack over each other, but because of the presence of the central backbone, their molecular stacking differs from that in the monomeric PDI crystal.[42,43] Such a different packing and thus different overlap of the π-orbitals was found to lead to a difference in ϕ of 70 ± 15 mV as measured by KPFM between P-PDI fibers and PDI nanocrystals, despite their very similar HOMO and LUMO levels.[44]

IV. Direct Exploration of Dynamic Complex Electronic Processes and Phenomena

In photovoltaic blends, the processes of photon adsorption and exciton splitting and the presence of opposite charges in the EA and ED phases lead to local changes in SP, which is called surface photovoltage ($SPV = SP_{light} - SP_{dark}$). Studies performed on bulk heterojunctions showed a strong correlation between SPV and morphology on the sub-micro-scale,[16,22,23] providing evidence that the presence of local heterogeneities, large-scale phase segregation, and defects reduces the photovoltaic performance of the donor−acceptor system. KPFM does not directly map exciton splitting and charge generation because the characteristic nanosecond time scales of these processes are beyond the time resolution of the technique.

KPFM maps the photoactivities under steady-state conditions, detecting the photocharges continuously generated and transferred into the EA LUMO and ED HOMO, respectively, which accumulate in different areas of the substrate. In general, the substrate plays an active role in the measured SP differences between EA and ED phases, which are usually ascribed to interface dipoles[22] or to band-bending due to diffusion of substrate charges into organic assemblies.[45]

In organic materials, the photogenerated excitons have a typical diffusion length of ca. 10 nm. KPFM can quantitatively monitor the substrate potential as well as the generated charges on such a scale as shown on thin blends of the ED (P3HT) with either monomeric PDI[24] or polymeric P-PDI[46] deposited on silica from $CHCl_3$ solutions.

For PDI, to unveil the role of the reciprocal space positions of the EA crystals and ED amorphous aggregate, a particular film was prepared with crystals of the EA either in direct contact with or distanced by several hundreds of nanometers from the ED aggregate (Figure 5a). All the PDI clusters, above 50 nm (Figure 5b), exhibit the same SP values before illumination (Figure 5c), whereas on illumination with white light (Figure 5d), only the clusters in contact with P3HT islands show a negative shift ($SPV_{PDI} < 0$). The isolated PDI and the substrate behave as spectators, because their potentials

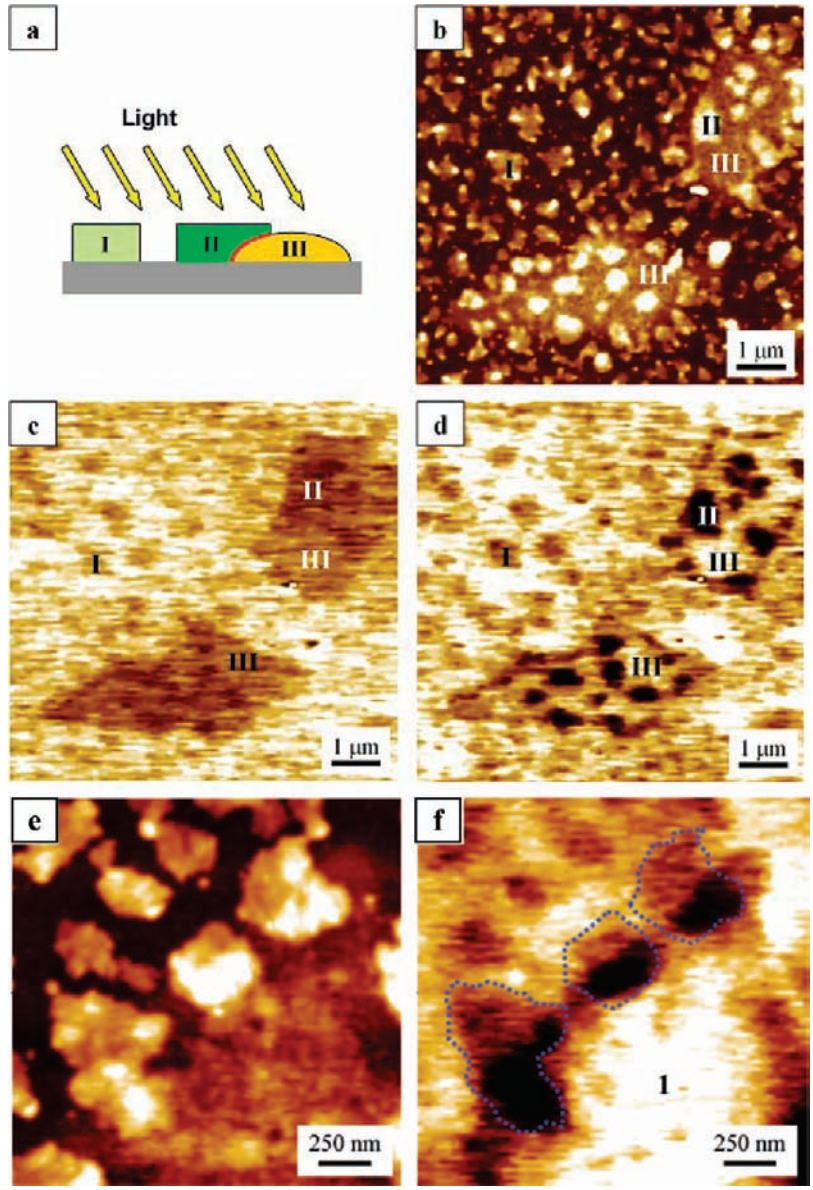

FIGURE 5. (a) Cartoon of illuminated P3HT/PDI blend. (b) AFM topography and the corresponding KPFM images under (c) no illumination and (d) illumination. PDI agglomerates are isolated (white arrows) or in contact (black arrows) with P3HT islands. (e) AFM topographic image shows in greater detail the PDI clusters marked by the dotted contours in panel f, the KPFM image. *Z*-ranges were (b) 20 nm, (c) 60 mV, (d) 37 mV, (e) 17 nm, and (f) 63 mV.[24]

remain approximately the same ($SPV_{PDI} \approx SPV_{P3HT} \approx 0$), whereas the P3HT SP increases ($SPV_{P3HT} > 0$).

The negative (positive) shift in SPV corresponds to an increase in electron (hole) density. Hence, only the EA aggregates in contact with the ED receive electrons compared with the pristine blend without illumination. The driving force for exciton splitting and charge separation derives from the different electron affinity of the EA and ED phases; because of this, significant charging was observed only for the PDI crystals in contact with the ED material (Figure 5e,f).

Taking into account the effective area, the SPV of PDI clusters in contact with P3HT amounts to -50 ± 11 mV due to the presence of photocharges amounting to only very few electrons (ca. 10).

Different behavior was observed when P3HT was blended with P-PDI. The two fiber-forming polymers assemble into interpenetrated bundles having a nanophase segregated character and featuring a high density of contact points (Figure 6a). The two phases and the substrate can be easily distinguished in the KPFM measurements without (Figure 6c) or with (Figure 6e) illumination, where the acceptor (black arrow) and donor (white arrow) properties are directly correlated with the material potential. The SP difference between the two phases increases when the sample is illuminated as in the PDI/P3HT

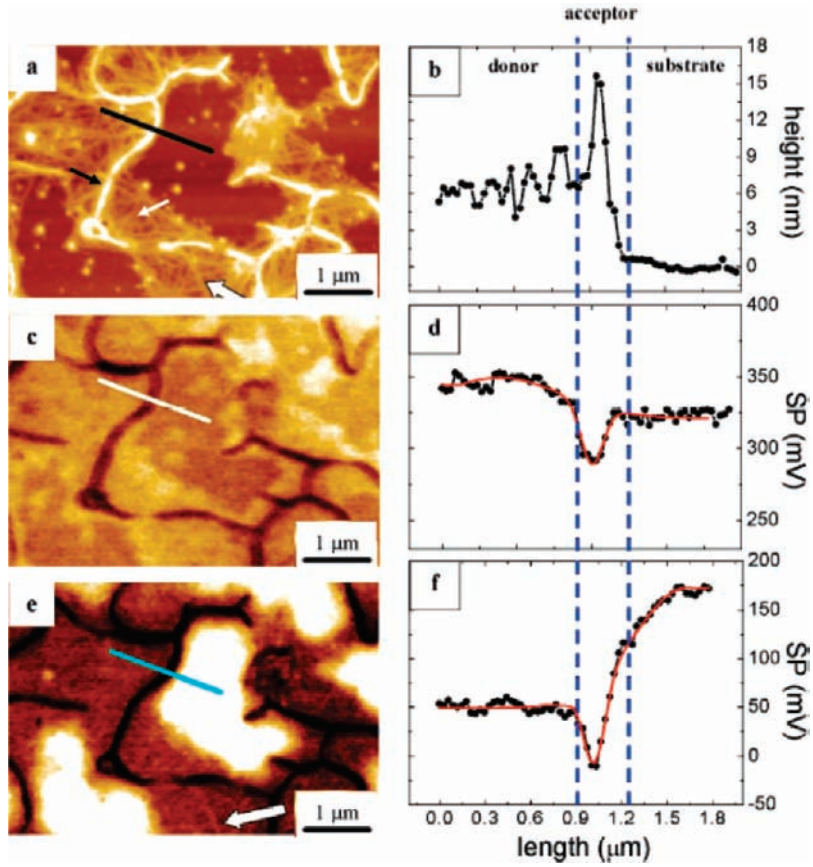

FIGURE 6. (a) AFM topography image of P-PDI/P3HT blend on silica and the corresponding KPFM images under (c) no illumination and (e) illumination. Panels b, d, and f are measured (black lines and circles) and simulated (red lines) profiles obtained by tracing the arbitrary lines in the corresponding images. *Z*-ranges were (a) 32 nm, (c) 120 mV, and (e) 120 mV.[46]

blend, with a further SP negative shift of the substrate being observed ($SPV_{silica} \approx -150$ mV).

For this "all-polymer" system, interconnectivity is much more extended than for the case of PDI/P3HT; consequently a more uniform charging of both EA and ED phases is observed, with the SP of P-PDI and P3HT being almost constant over different surface areas.

The different SP behavior of silica cannot be ascribed to experimental artifacts, showing once again the strong interaction existing between the electrical and the morphological properties at the nanoscale.

A very attractive yet still poorly explored field of KPFM application is the electric potential measurement of biological systems. Proteins, DNA, and biological systems in general, have relatively much larger sizes (from tens of nanometers up to several micrometers), as well as possessing well-defined structures; their biological activity relies upon the presence and creation of highly localized charges within their structure, making them good candidates for KPFM analysis.

By analogy with the aforementioned KPFM studies of photovoltaic materials, KPFM was employed to study the photosynthetic activity of single photosystem I (PSI) reaction centers, that is, one of the molecular components of green plants, immobilized both on gold and on patterned glass substrates.[47] The adsorbed light triggers electron-transfer reactions across the reaction center complex, generating a voltage, which powers the energetically uphill reactions of photosynthesis. Both the PSI size (45 nm) and the voltage shift (~1 V) are suitable for real-time KPFM mapping of biological activity. A major issue in measuring these kinds of proteic nano-objects is their high electrical anisotropy, with charges moving from one side of the PSI to the other upon illumination. Thus, to obtain reliable and reproducible measurements, the orientation of the PSI on the substrate must be controlled. This can be done by functionalizing the gold substrate with mercaptoethanol, which results in a preferential adsorption of the PSI with electron acceptor side up.

KPFM studies of the biological activity of micrometric assemblies are typically performed on dry samples.[48] This represents a major problem since it is crucial to maintain such biosystems in a wet environment, that is, at least with a thin water layer between probe and sample. Experimental artifacts due to water polarization induced by the charged probe cannot be neglected, but a complete description of this water con-

tribution to the measured SP is still lacking and the improvement of models and viable computational procedures to extrapolate quantitative information in wet systems is necessary. Stuart and co-workers[49] measured the SPV change of bacteriorhodopsin at different pH values, allowing the study of the mechanism of photocharge generation on the external side of the *Halobacterium* cellular membrane and paving the way toward possible applications for optically coupled FETs, high-speed photodetectors, and artificial retinas.

V. Conclusions and Future Perspectives

KPFM is a very powerful tool for real space exploration of the correlation between structural and electrical/electronic properties of a wide range of systems, ranging from working nanodevices to processes in biological structures. Such information will be fundamental for the optimization of functional materials and will open up a large range of nanoscale applications.

Despite the high lateral and voltage resolution of KPFM, one major challenge is to develop models for describing probe−sample interactions and viable computational procedures to extrapolate quantitative information on electrical and electronic properties down to the 1−10 nm scale. Further improvements in KPFM include enhancement of the time resolution, which would allow the study of dynamic properties and system response under the effect of different external stimuli, such as light irradiation or mechanical stress.

Nanoscale electrical and electronic characterizations of functional materials are continuously improving. In the light of its applicability to a wide range of sample types, this technique promises a decisive contribution to the design and fabrication of hybrid nanosystems and nanodevices.

Dedicated to Professor Carlo Taliani on the occasion of his 65th birthday. We thank Dr. Derek Jones for his comments on the manuscript. This work was supported by the ESF-SONS2-SUPRAMATES, the NanoSci-E+ project SENSORS, the EC Marie Curie RTN THREADMILL (MRTN-CT-2006-036040), the EC FP7 ONE-P large-scale project no. 212311, the Regione Emilia-Romagna PRIITT Nanofaber Net-Lab, and the International Center for Frontier Research in Chemistry (FRC).

BIOGRAPHICAL INFORMATION

Andrea Liscio (Roma, Italy, 1975) received his Ph.D. in 2004 in the Institute of Inorganic Methodologies and Plasmas of the CNR, Roma, for his work on electron-surface modeling to study surface and organic thin film electronic systems using unconventional electronic spectroscopies. Since 2005, he has been a postdoctoral research fellow at ISOF-CNR, Bologna. His current research interest is the use of scanning probe microscopies beyond imaging to unravel the correlation between structural and electronic properties in thin films and supramolecular nanostructures for organic opto-electronics.

Vincenzo Palermo (S. Severo, Italy, 1972) performed his Ph.D. at ISOF-CNR, Bologna, working on STM characterization of silicon nanostructures for microelectronics. He has worked in the groups of Prof. Y. K. Levine (University of Utrecht, The Netherlands) and Prof. R. A. Wolkow (National Research Council, Canada). His main research interests involve the structural and electronic characterization of organic semiconductor nanostructures using scanning probe microscopies. He received the Young Scientist Award at EMRS (2003), best Ph.D. award at ECME (2005), and the Italian Society for Microscopic Sciences (SISM) award (2006). He is presently a research scientist at ISOF-CNR.

Paolo Samorì (Imola, Italy, 1971) is full professor (PR1) at the Institut de Science et d'Ingénierie Supramoléculaires (ISIS) of the Université de Strasbourg (UdS), and he is Director of the Nanochemistry Laboratory at ISIS. In 2000, he received his Ph.D. in Chemistry from the Humboldt University Berlin (Prof. J. P. Rabe). He was permanent research scientist at Istituto per la Sintesi Organica e la Fotoreattività (ISOF) of the Consiglio Nazionale delle Ricerche (CNR) of Bologna from 2001 to 2008 and Visiting Professor at ISIS from 2003 to 2008. He has published >115 papers on the application of SPMs beyond imaging, hierarchical self-assembly of hybrid architectures at surfaces, supramolecular electronics, and the fabrication of molecular-scale nanodevices. He has been awarded various prizes, including the young scientist awards at EMRS (1998) and MRS (2000), as well as the IUPAC Prize for Young Chemists 2001, the "Vincenzo Caglioti" award 2006 granted by the Accademia Nazionale dei Lincei, and the "Nicolò Copernico" award 2009 (Italy) for his discoveries in the field of nanoscience and nanotechnology.

FOOTNOTES

*To whom correspondence should be addressed. E-mail addresses: palermo@isof.cnr.it; samori@isis-ulp.org.

REFERENCES

1 Nonnenmacher, M.; Oboyle, M. P.; Wickramasinghe, H. K. Kelvin Probe Force Microscopy. *Appl. Phys. Lett.* **1991**, *58*, 2921–2923.

2 Weaver, J. M. R.; Abraham, D. W. High-Resolution Atomic Force Microscopy Potentiometry. *J. Vac. Sci. Technol., B* **1991**, *9*, 1559–1561.

3 Kelvin, L. Contact Electricity of Metals. *Philos. Mag.* **1898**, *46*, 82–120.

4 Zisman, W. A. A New Method of Measuring Contact Potential Differences in Metals. *Rev. Sci. Instrum.* **1932**, *3*, 367–370.

5 Samorì, P. Exploring Supramolecular Interactions and Architectures by Scanning Force Microscopies. *Chem. Soc. Rev.* **2005**, *34*, 551–561.

6 The work function ϕ is the minimal energy required to remove an electron from the electronic ground state in a given material. It is defined as the difference between the vacuum level (i.e. the energy of an electron at rest far from the influence of the potential of the solid) and the Fermi energy.

7 Kalinin, S. V.; Bonnell, D. A. Local Potential and Polarization Screening on Ferroelectric Surfaces. *Phys. Rev. B* **2001**, *63*, 125411.

8 Palermo, V.; Liscio, A.; Palma, M.; Surin, M.; Lazzaroni, R.; Samorì, P. Exploring Nanoscale Electrical and Electronic Properties of Organic and Polymeric Functional Materials by Atomic Force Microscopy Based Approaches. *Chem. Commun.* **2007**, 3326–3337.

9 Meoded, T.; Shikler, R.; Fried, N.; Rosenwaks, Y. Direct Measurement of Minority Carriers Diffusion Length Using Kelvin Probe Force Microscopy. *Appl. Phys. Lett.* **1999**, *75*, 2435–2437.

10 Palermo, V.; Palma, M.; Tomovic, Z.; Watson, M. D.; Friedlein, R.; Müllen, K.; Samorì, P. Influence of the Molecular Order on the Local Work Function of Nanographene Architectures: A Kelvin-Probe Force Microscopy Study. *ChemPhysChem* **2005**, *6*, 2371–2375.

11 Lu, J.; Eng, L.; Bennewitz, R.; Meyer, E.; Guntherodt, H. J.; Delamarche, E.; Scandella, L. Surface Potential Studies of Self-Assembling Monolayers Using Kelvin Probe Force Microscopy. *Surf. Interface Anal.* **1999**, *27*, 368–373.

12 Gil, A.; de Pablo, P. J.; Colchero, J.; Gomez-Herrero, J.; Baro, A. M. Electrostatic Scanning Force Microscopy Images of Long Molecules: Single-Walled Carbon Nanotubes and DNA. *Nanotechnology* **2002**, *13*, 309–313.

13 Kwak, K. J.; Yoda, S.; Fujihira, M. Observation of Stretched Single DNA Molecules by Kelvin Probe Force Microscopy. *Appl. Surf. Sci.* **2003**, *210*, 73–78.

14 Chotsuwan, C.; Blackstock, S. C. Single Molecule Charging by Atomic Force Microscopy. *J. Am. Chem. Soc.* **2008**, *130*, 12556–12557.

15 Bürgi, L.; Sirringhaus, H.; Friend, R. H. Noncontact Potentiometry of Polymer Field-Effect Transistors. *Appl. Phys. Lett.* **2002**, *80*, 2913–2915.

16 Hoppe, H.; Glatzel, T.; Niggemann, M.; Hinsch, A.; Lux-Steiner, M. C.; Sariciftci, N. S. Kelvin Probe Force Microscopy Study on Conjugated Polymer/Fullerene Bulk Heterojunction Organic Solar Cells. *Nano Lett.* **2005**, *5*, 269–274.

17 Puntambekar, K. P.; Pesavento, P. V.; Frisbie, C. D. Surface Potential Profiling and Contact Resistance Measurements on Operating Pentacene Thin-Film Transistors by Kelvin Probe Force Microscopy. *Appl. Phys. Lett.* **2003**, *83*, 5539–5541.

18 Ganzorig, C.; Kwak, K. J.; Yagi, K.; Fujihira, M. Fine Tuning Work Function of Indium Tin Oxide by Surface Molecular Design: Enhanced Hole Injection in Organic Electroluminescent Devices. *Appl. Phys. Lett.* **2001**, *79*, 272–274.

19 Sakomura, M.; Fujihira, M. Scanning Maxwell Stress Microscopy of Photo-Induced Charge Separation in A-S-D Triad Monolayers. *J. Photochem. Photobiol., A* **2004**, *166*, 45–56.

20 Jaquith, M. J.; Anthony, J. E.; Marohn, J. A. Long-Lived Charge Traps in Functionalized Pentacene and Anthradithiophene Studied by Time-Resolved Electric Force Microscopy. *J. Mater. Chem.* **2009**, *19*, 6116–6123.

21 Coffey, D. C.; Ginger, D. S. Time-Resolved Electrostatic Force Microscopy of Polymer Solar Cells. *Nat. Mater.* **2006**, *5*, 735–740.

22 Chiesa, M.; Bürgi, L.; Kim, J. S.; Shikler, R.; Friend, R. H.; Sirringhaus, H. Correlation between Surface Photovoltage and Blend Morphology in Polyfluorene-Based Photodiodes. *Nano Lett.* **2005**, *5*, 559–563.

23 Palermo, V.; Ridolfi, G.; Talarico, A. M.; Favaretto, L.; Barbarella, G.; Camaioni, N.; Samorì, P. A Kelvin Probe Force Microscopy Study of the Photogeneration of Surface Charges in All-Thiophene Photovoltaic Blends. *Adv. Funct. Mater.* **2007**, *17*, 472–478.

24 Liscio, A.; De Luca, G.; Nolde, F.; Palermo, V.; Müllen, K.; Samorì, P. Photovoltaic Charge Generation Visualized at the Nanoscale: A Proof of Principle. *J. Am. Chem. Soc.* **2008**, *130*, 780–781.

25 Bürgi, L.; Friend, R. H.; Sirringhaus, H. Formation of the Accumulation Layer in Polymer Field-Effect Transistors. *Appl. Phys. Lett.* **2003**, *82*, 1482–1484.

26 Nichols, J. A.; Gundlach, D. J.; Jackson, T. N. Potential Imaging of Pentacene Organic Thin-Film Transistors. *Appl. Phys. Lett.* **2003**, *83*, 2366–2368.

27 Fujihira, M. Kelvin Probe Force Microscopy of Molecular Surfaces. *Annu. Rev. Mater. Sci.* **1999**, *29*, 353–380.

28 Palermo, V.; Palma, M.; Samorì, P. Electronic Characterization of Organic Thin Films by Kelvin Probe Force Microscopy. *Adv. Mater.* **2006**, *18*, 145–164.

29 Love, J. C.; Estroff, L. A.; Kriebel, J. K.; Nuzzo, R. G.; Whitesides, G. M. Self-Assembled Monolayers of Thiolates on Metals As a Form of Nanotechnology. *Chem. Rev.* **2005**, *105*, 1103–1169.

30 Samorì, P. Scanning Probe Microscopies beyond Imaging. *J. Mater. Chem.* **2004**, *14*, 1353–1366.

31 Kalinin, S. V.; Gruverman, A. *SPM, Electrical and Electromechanical Phenomena at the Nanoscale*; Springer Verlag: Berlin, 2006.

32 Ishii, H.; Sugiyama, K.; Ito, E.; Seki, K. Energy Level Alignment and Interfacial Electronic Structures at Organic/Metal and Organic/Organic Interfaces. *Adv. Mater.* **1999**, *11*, 605–625.

33 Heimel, G.; Romaner, L.; Zojer, E.; Brédas, J. L. The Interface Energetics of Self-Assembled Monolayers on Metals. *Acc. Chem. Res.* **2008**, *41*, 721–729.

34 Lee, M.; Lee, W.; Prinz, F. B. Geometric Artefact Suppressed Surface Potential Measurements. *Nanotechnology* **2006**, *17*, 3728–3733.

35 Liscio, A.; Palermo, V.; Gentilini, D.; Nolde, F.; Müllen, K.; Samorì, P. Quantitative Measurement of the Local Surface Potential of Pi-Conjugated Nanostructures: A Kelvin Probe Force Microscopy Study. *Adv. Funct. Mater.* **2006**, *16*, 1407–1416.

36 Colchero, J.; Gil, A.; Baro, A. M. Resolution Enhancement and Improved Data Interpretation in Electrostatic Force Microscopy. *Phys. Rev. B* **2001**, *64*, 245403.

37 Strassburg, E.; Boag, A.; Rosenwaks, Y. Reconstruction of Electrostatic Force Microscopy Images. *Rev. Sci. Instrum.* **2005**, *76*, 083705.

38 Charrier, D. S. H.; Kemerink, M.; SmalbrLigge, B. E.; de Vries, T.; Janssen, R. A. J. Real versus Measured Surface Potentials in Scanning Kelvin Probe Microscopy. *ACS Nano* **2008**, *2*, 622–626.

39 Liscio, A.; Palermo, V.; Samorì, P. Probing Local Surface Potential of Quasi-One-Dimensional Systems: A KPFM Study of P3HT Nanofibers. *Adv. Funct. Mater.* **2008**, *18*, 907–914.

40 Liscio, A.; Palermo, V.; Müllen, K.; Samorì, P. Tip−Sample Interactions in Kelvin Probe Force Microscopy: Quantitative Measurement of the Local Surface Potential. *J. Phys. Chem. C* **2008**, *112*, 17368–17377.

41 Brédas, J. L.; Calbert, J. P.; da Silva, D. A.; Cornil, J. Organic Semiconductors: A Theoretical Characterization of the Basic Parameters Governing Charge Transport. *Proc. Natl. Acad. Sci. U.S.A.* **2002**, *99*, 5804–5809.

42 Schwartz, E.; Palermo, V.; Finlayson, C. E.; Huang, Y. S.; Otten, M. B. L.; Liscio, A.; Trapani, S.; Gonzalez-Valls, I.; Brocorens, P.; Cornelissen, J. J. L. M.; Peneva, K.; Müllen, K.; Spano, F. C.; Yartsev, A.; Westenhoff, S.; Friend, R. H.; Beljonne, D.; Nolte, R. J. M.; Samorì, P.; Rowan, A. E. "Helter-Skelter-Like" Perylene Polyisocyanopeptides. *Chem.—Eur. J.* **2009**, *15*, 2536–2547.

43 Struijk, C. W.; Sieval, A. B.; Dakhorst, J. E. J.; van Dijk, M.; Kimkes, P.; Koehorst, R. B. M.; Donker, H.; Schaafsma, T. J.; Picken, S. J.; van de Craats, A. M.; Warman, J. M.; Zuilhof, H.; Sudholter, E. J. R. Liquid Crystalline Perylene Diimides: Architecture and Charge Carrier Mobilities. *J. Am. Chem. Soc.* **2000**, *122*, 11057–11066.

44 Hernando, J.; de Witte, P. A. J.; van Dijk, E.; Korterik, J.; Nolte, R. J. M.; Rowan, A. E.; Garcia-Parajo, M. F.; van Hulst, N. F. Investigation of Perylene Photonic Wires by Combined Single-Molecule Fluorescence and Atomic Force Microscopy. *Angew. Chem., Int. Ed.* **2004**, *43*, 4045–4049.

45 Maturova, K.; Kemerink, M.; Wienk, M. M.; Charrier, D. S. H.; Janssen, R. A. J. Scanning Kelvin Probe Microscopy on Bulk Heterojunction Polymer Blends. *Adv. Funct. Mater.* **2009**, *19*, 1379–1386.

46 Palermo, V.; Otten, M. B. J.; Liscio, A.; Schwartz, E.; de Witte, P. A. J.; Castriciano, M. A.; Wienk, M. M.; Nolde, F.; De Luca, G.; Cornelissen, J. J. L. M.; Janssen, R. A. J.; Müllen, K.; Rowan, A. E.; Nolte, R. J. M.; Samorì, P. The Relationship between Nanoscale Architecture and Function in Photovoltaic Multichromophoric Arrays as Visualized by Kelvin Probe Force Microscopy. *J. Am. Chem. Soc.* **2008**, *130*, 14605–14614.

47 Lee, I.; Lee, J. W.; Stubna, A.; Greenbaum, E. Measurement of Electrostatic Potentials above Oriented Single Photosynthetic Reaction Centers. *J. Phys. Chem. B* **2000**, *104*, 2439–2443.

48 Sinensky, A. K.; Belcher, A. M. Label-Free and High-Resolution Protein/DNA Nanoarray Analysis Using Kelvin Probe Force Microscopy. *Nat. Nanotechnol.* **2007**, *2*, 653–659.

49 Lee, I.; Greenbaum, E.; Budy, S.; Hillebrecht, J. R.; Birge, R. R.; Stuart, J. A. Photoinduced Surface Potential Change of Bacteriorhodopsin Mutant D96N Measured by Scanning Surface Potential Microscopy. *J. Phys. Chem. B* **2006**, *110*, 10982–10990.